Express Polymer Letters Vol.17, No.10 (2023) 992–1006
Available online at www.expresspolymlett.com
https://doi.org/10.3144/expresspolymlett.2023.74

Research article

Sustainable polymers and sisal fibers based green composites: A detailed characterization and analysis

Karri Santhosh Kumar[1], *Sandeep Gairola*[2], *Inderdeep Singh*[1,2*]

[1]Mechanical and Industrial Engineering Department, Indian Institute of Technology Roorkee, Uttarakhand, India
[2]Centre of Excellence in Disaster Mitigation and Management, Indian Institute of Technology Roorkee, Uttarakhand, India

Received 11 April 2023; accepted in revised form 22 June 2023

Abstract. In the global pursuit of using sustainable constituents for developing composite materials, the current investigation has paid particular attention to the most promising biopolymers, such as poly(lactic acid) (PLA) and bio-based poly(butylene succinate) (bio PBS). The research endeavor emphasizes a comparative assessment of short sisal fiber (SF) reinforced (10, 20, and 30 wt%) PLA and bio PBS biocomposites. The analysis and discussion have been reported for the thermal, mechanical, crystallinity, and dynamic mechanical behavior of developed composite materials. Based on mechanical properties, the optimal fiber loading for SF/PLA and SF/bio PBS biocomposites was 20 and 30 wt%, respectively. The developed composites have shown a considerable improvement in crystallinity of 17.88 and 41.13% at 20 and 30 wt% of fiber loading in SF/PLA and SF/bio PBS, respectively. The maximum storage modulus values of 14.23 GPa (20SF/PLA) and 11.74 GPa (30SF/bio PBS) were observed. The loss modulus of the SF/PLA and SF/bio PBS composites was around 74 and 89% higher than the loss modulus of the PLA and the bio PBS matrix, respectively. Overall, composites fabricated with bio PBS (SF/bio PBS) have shown better crystallinity, thermal stability, and ease of processing than SF/PLA composites.

Keywords: *biodegradable polymers, biocomposites, mechanical properties, thermal properties, degree of crystallinity*

1. Introduction

Polymers derived from renewable sources have recently drawn a lot of attention in replacing the traditional petrochemical-derived and non-degradable polymers due to problematic plastic pollution and the rising oil price [1]. Among the most promising biodegradable polymers is bio-based polybutylene succinate (bio PBS), which has high ductility and melt processing capabilities, making it appropriate for various industries, including flexible packaging, agriculture, and consumer goods. PBS is a polyester made of poly-condensing succinic acid and 1,4-butanediol. Until recently, both PBS monomers were typically produced by several processes that began with petrochemical compounds. These monomers can also be made by fermenting agricultural or industrial wastes or other renewable resources (bio-based) [2–4]; the Biomass content of PBS accounts for 80% of its total composition [5]. Similarly, lactic acid is converted into PLA through ring-opening or grafting polymerization in plants that contain starch, such as corn and cassava. It is also a thermoplastic polymer with superior strength and transparency [6]. However, drawbacks such as brittleness limit its processability, making it unsuitable for use in the packaging industries, especially where high ductility is required [7, 8].

The predominant disadvantages of biopolymers are high cost and limited performance. The high price is due to the low production volume of biopolymers and the lack of knowledge. Therefore, biopolymers are often reinforced with natural fibers to develop novel composite materials. Combining natural fibers addresses the properties and cost of the composites [9,

*Corresponding author, e-mail: inderdeep.singh@me.iitr.ac.in

10]. The sisal fibers produced from the leaves of sisal plants have been investigated in the current study as a natural, cost-effective filler within bio PBS and PLA at various weight percentages. Sisal fiber (SF) is one of the most widely used natural fibers. Nearly 4.5 million tons of SFs are produced every year throughout the world. A sisal plant yields 200–250 leaves, each carrying more than a thousand fiber bundles with a fiber content of 4% [11]. It has a rough surface due to its coarse grain structure, high strength, and high water absorption capacity [12, 13]. SFs were chosen due to their yearly large quantity availability, compatibility with biopolymers (due to their coarse grain structure), and affordability. Due to their superior mechanical performance and relative stability, PLA and bio PBS may eventually replace conventional thermoplastic polymers. Interestingly, the melting temperatures of these two biodegradable polymers (bio PBS and PLA) are below 200 °C, enabling the production of biocomposites without damaging sisal fibers [14].

Ngaowthong *et al*. [15] used a co-rotated twin screw extruder to develop composites made of sisal fiber, polypropylene, and PLA. The incorporation of sisal fiber enhanced the tensile modulus and percentage crystallinity of composites. Zhu *et al*. [16] studied the effect of the chemical composition of fibers on the tensile strength of SF and the interfacial strength between SFs and PLA. The results showed that the optimal ratio of fiber constituents (cellulose, hemicellulose, and lignin) was suitable for the tensile strength of SF and the interfacial strength between SF and PLA. Feng *et al*. [17] established a technique to assess the rheological characteristics of SF/PBS composites and, after mixing, estimated the aspect ratio of SFs. The results indicate that shear thinning is more pronounced with increasing SF content, because of disentanglement, breakage, and orientation of SFs. During the extrusion process, when fiber content increases, the number of fibers within the given volume increases, which leads to increased friction and shearing action between the fibers, resulting in decreased fiber length due to fiber breakage and subsequently leading to decreased aspect ratio. Bajpai *et al*. [18] developed composites with natural fibers with polypropylene and PLA matrices and assessed their mechanical and morphological characteristics. PLA/sisal fiber composites showed superior mechanical properties.

Yan *et al*. [19] reported crystallization and dynamic mechanical analysis (DMA) behavior of coir fiber/ PBS biocomposites with 20 and 40 wt% fiber content. X-ray diffraction (XRD) shows identical crystal forms of pure PBS and coir fiber/ PBS composites. Storage modulus significantly increased in coir fiber/ PBS composites. Li *et al*. [20] evaluated the mechanical characteristics and crystallinity of PBS/basalt fiber biocomposites. Composites were made with different fiber content using a twin screw extruder and injection molding. Adding basalt fiber enhanced the mechanical properties and thermal stability of composites. Due to the negligible nucleation impact of basalt fiber, the crystallization of PBS in composites does not alter. Samouh *et al*. [21] evaluated the mechanical and thermal properties and DMA behavior of PLA/sisal fiber biocomposites with various fiber weight fractions. The mechanical and DMA behavior of biocomposites improves with an increase in the reinforcing rate. Increased sisal fiber content improved the crystallinity in the matrix because the fibers serve as PLA nucleating agents.

In the last two decades, there has been noteworthy research in the field of natural fiber-reinforced biodegradable composites. However, most literature focused on individual biopolymer-based composites or biopolymer blends. A considerable volume of research has focused on PLA-based composites despite their disadvantages as compared to other biodegradable polymers. There has been limited research on other biodegradable polymers, such as PBS, poly(3-hydroxybutyrate-*co*-3-hydroxyvalerate) (PHBV), and poly(butylene adipate-*co*-terephthalate) (PBAT). The present research investigation aims to develop and conduct a comparative assessment of untreated short sisal fiber-reinforced (10, 20, and 30 wt%) PLA/ bio PBS matrix sustainable composites. The mechanical, thermal, crystallinity and morphological characteristics of developed composites have been investigated in detail and reported.

2. Materials and methodology

2.1. Materials

Raw sisal fibers were procured from the Women's Development Organisation, Dehradun, India. SFs were shredded into short fibers with an average 3–6 mm length. The PLA (grade 3052D) was purchased from Nature Tech. India Pvt. Ltd. in Chennai, India, in pellets form (density, $\rho = 1.24$ g/cm^3, melt flow

rate, *MFR* = 14 g/10 min (210 °C, 2.16 kg)). Bio PBS (grade: FZ71PB) was procured from Tanhim Enterprises Pvt. Ltd., Greater Noida, India, in the form of pellets (ρ =1.26 g/cm^3, *MFR* = 22 g/10 min (190 °C, 2.16 kg)).

2.2. Fiber characterization

Single fiber strength tests were performed using Instron 5982 following ASTM D3822-14 with a fixed gauge length of 30 mm and a crosshead speed of 0.5 mm/min. The SF strands were fastened on cardboard paper with the help of an adhesive. The fiber diameter was obtained by averaging five observations along the fiber length using a stereo microscope with the help of VUE 2014 software (with a magnification factor of 50). The surface of an untreated sisal fiber was analyzed using a Field Emission Scanning Electron Microscope (FESEM) (Make: ZEISS, Model: Gemini 1). The weight percentage of organic elements in SF was determined using the energy dispersive spectroscope (EDS). The thermogravimetric analyzer (TGA) (EXSTAR 6300) was used to examine the thermal stability and degradation behavior of fibers. The maximum test temperature and the heating rate were 700 °C and 10 °C/min, respectively, and analysis was conducted in a nitrogen atmosphere (200 ml/min).

2.3. Fabrication of composite specimens

Before using sisal fibers for blending, fibers were drenched in tap water for 24 hours to get rid of dirt and pith from the fiber surface and, thereafter, dried under sunlight for 48 hours to remove moisture from the fibers. The fibers were heated to 80 °C in an air-circulated oven for 6 hours. PLA and bio PBS were dried in an oven at 50 °C for 8 hours and blended with SF (10, 20, 30 wt%) using a single screw extruder (Make: Sai Extrumech Model: SAI-25) at a temperature of 165 and 135 °C, respectively, and extruder speed of 45 rpm. The blended composite strands were passed through the water bath and pelletized into an average length of 4–5 mm.

The fabrication process of biocomposites using extrusion-injection molding is depicted in Figure 1 and the nomenclature for the same is shown in Table 1.

Extruded pellets were used in the injection molding machine (Make: Electronica Model: ENDURA-60) to make final specimens in accordance with ASTM standards. The processing temperature values for heaters along the barrel (from hopper to nozzle) were optimized from pilot experiments. The temperatures of respective zones are 165–170–175–180 °C (PLA/SF composites) and 155–155–160–155 °C (Bio PBS/SF composites).

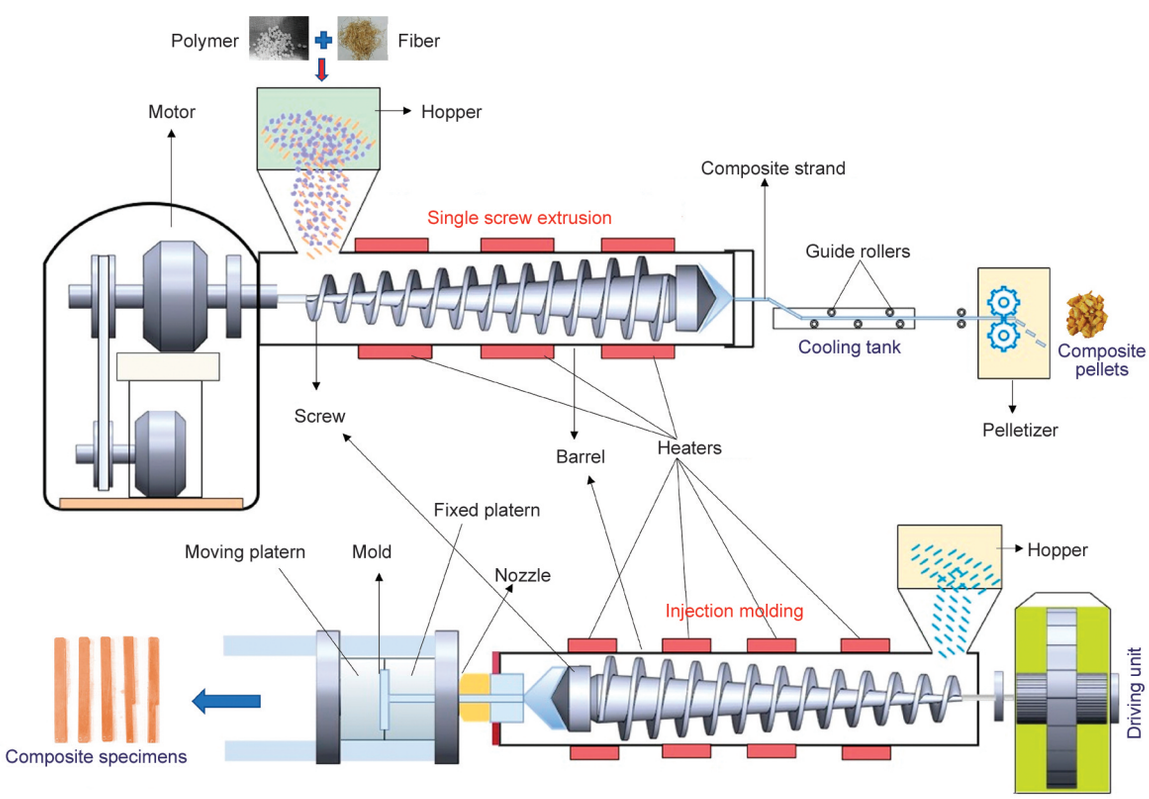

Figure 1. Schematic diagram showing processing of composite specimens.

Table 1. Nomenclature for specimens prepared by extrusion-injection molding.

Specimen name	Nomenclature
PLA	Poly(lactic acid)
Bio PBS	Bio based poly(butylene succinate)
SF	Sisal fiber
USF	Untreated sisal fiber
10SF	10 wt% sisal fiber loading
20SF	20 wt% sisal fiber loading
30SF	30 wt% sisal fiber loading
SF/PLA or SF_PLA	Sisal fiber-based PLA composite.
SF/bio PBS or SF_bio PBS	Sisal fiber-based bio PBS composite.
EIM	Extrusion-injection molding

2.4. Characterization of biocomposites

The optimum weight percentage of fibers in the developed biocomposites and mechanical behavior were evaluated and compared. The thermal and morphological properties and crystallinity of fabricated composites were assessed and compared. A universal testing machine (UTM) (Make: Instron, Type: 5982) with a 100 kN capacity was used to evaluate the tensile and flexural strength. According to the ASTM D3039M-14, tensile tests were carried out at a crosshead speed of 2 mm/min and a gauge length of 50 mm, respectively. According to ASTM D790-10, flexural tests were performed using a three-point bending fixture with a crosshead speed of 2 mm/min and 60 mm for the span length. The impact test employed a low-energy pendulum impact tester (Tinius Olsen-IT504) employing the ASTM D256-10 standard. The fractured surface of damaged samples after tensile testing was examined by SEM micrographs using the FESEM set-up. The thermal degradation characteristics of developed biodegradable polymer composites were measured by a thermogravimetric analyzer (Make: EXSTAR 6300). Under the nitrogen atmosphere, 10 mg samples were heated at 10 °C/min to 600 °C. The DMA (Make: NETZSCH, Model: DMA 242 C) was undertaken to understand the potential effects of SF loading on the visco-elastic response of composites and to examine the effectiveness of developed biocomposites under dynamic loading. In the three-point bending mode, samples with dimensions of 50×12×3 mm were tested as per ASTM D5023-15. DMA scans were performed at a ramping temperature of 2 °C/min, ranging from –45 to 90 °C, and a frequency of 1 Hz was used.

A thin film X-ray diffractometer (Make: Smart Lab Model: Rigaku) was used to analyze the amorphous and crystalline phases of fabricated samples. The sample's crystallinity was calculated using Equation (1) [22]:

$$\text{Crystallinity}\,[\%] = \frac{\text{Crystalline area}}{\text{Total area under the curve}} \cdot 100 \quad (1)$$

3. Results and discussion

3.1. Morphological examination of fibers

In scanning electron microscopy (SEM), an electron beam produces a magnified image of solid inorganic materials for microanalysis. Figure 2 portray the surface of SFs. Figure 2a shows the surface roughness of longitudinal SF, and Figure 2c reveals the presence of impurities and waxy cuticles [23, 24]. The parenchyma cells can be seen in Figure 2b [25].

3.2. Fiber strength test

The stress-strain behavior of untreated SF is shown in Figure 3. Stress-strain curves of fibers revealed minor extension after achieving peak strength value followed by brittle fracture. The extension after peak may be attributed to the load withstood by the intact fibrils that comprise the lignocellulosic fibers. The waviness in the curve may be attributed to surface roughness, waxy cuticles, and impurities on the surface of untreated SFs. Experimental outcomes established that the tensile behavior of fiber varied due to the variation in fiber diameter. The average tensile strength and modulus were determined as 235±54 MPa and 6.332±0.05 GPa, respectively.

3.3. Thermal analysis of fibers

Figure 4 depict the thermogravimetric (TG) and differential thermogravimetric (DTG) curves of SF, revealing the thermal degradation behavior of fibers. Thermogravimetric analysis (TGA) shows that the weight of the fibers decreases as the temperature increases. Initial degradation observed between 30 and 130 °C can be attributed to the moisture removal from the fibers. The second stage of degradation is due to the pyrolysis of cellulose and hemicellulosic content of fibers, which can be observed between 130 and 380 °C. Removal of lignin compounds from the surface of fibers due to pyrolysis was the reason

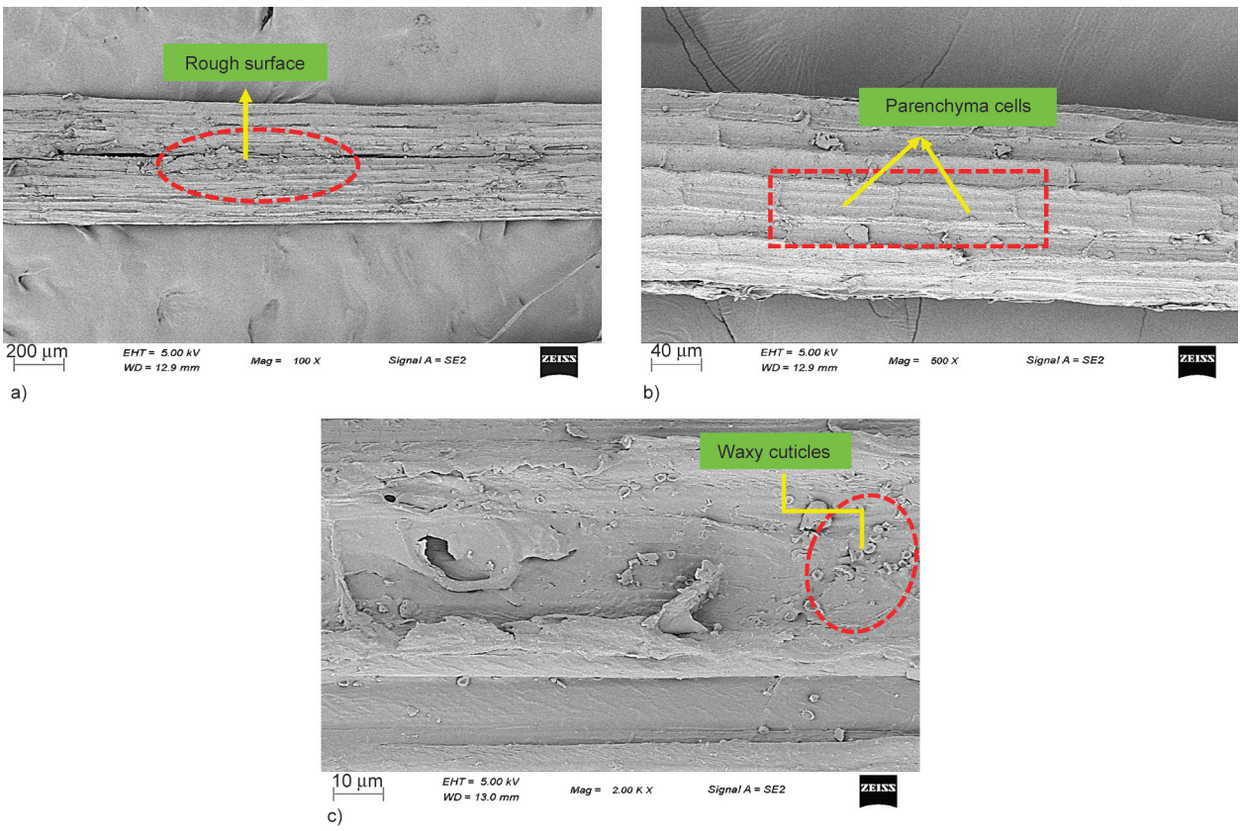

Figure 2. SEM images of untreated sisal fiber at different magnifications: a) 100×, b) 500×, c) 2000×.

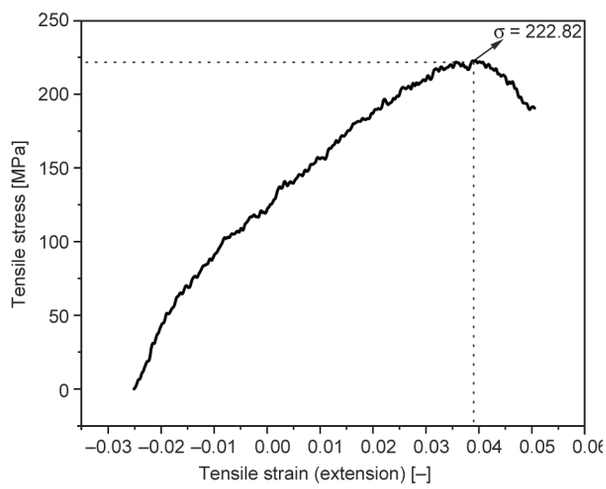

Figure 3. Typical stress-strain curve of USF.

for the third phase of thermal degradation of SFs, which was observed between 350 and 700 °C [25]. Figure 4b shows the DTG peaks for each step of degradation indicated by the TGA curves. The peaks of the DTG curve describe the weight loss rate [µg/min] against temperature. The degradation peak around 65 °C represented moisture evaporation from sisal fibers when heated. The degradation peak around 290 °C shows the thermal breakdown of hemicellulose. A maximum weight loss of 1.3 mg/min around 356 °C can be observed because of the pyrolysis of the cellulosic component of the fibers [25, 26].

3.4. Mechanical properties of biocomposites

3.4.1. Tensile properties

The effect of fiber content on the mechanical properties of developed biocomposites has been analyzed and summarized in Figure 5, and values are tabulated in Table 2. According to Figure 5a, the tensile strength of PLA/SF composites increased as the sisal fiber weight percentage increased to 20 wt% (45.12 MPa) and thereafter, reduced to 39.72 MPa at 30 wt% fiber concentration. The decrease in tensile strength after achieving the maximum value may be attributed to fiber agglomeration, which minimizes the fiber-matrix interfacial surface interaction in composites. Subsequently, the applied load is not effectively transferred from the matrix to the stiff fibers. Adding more fibers also causes non-uniform fiber dispersion in the PLA matrix [27, 28]. In the case of bio PBS/SF composites, the tensile strength decreased initially; thereafter, it was found to increase, with a maximum value of 29.12 MPa at 30 wt% of fiber loading. Adding SFs increased the strength of SF/bio PBS composites due to the uniform distribution of SFs that enable better

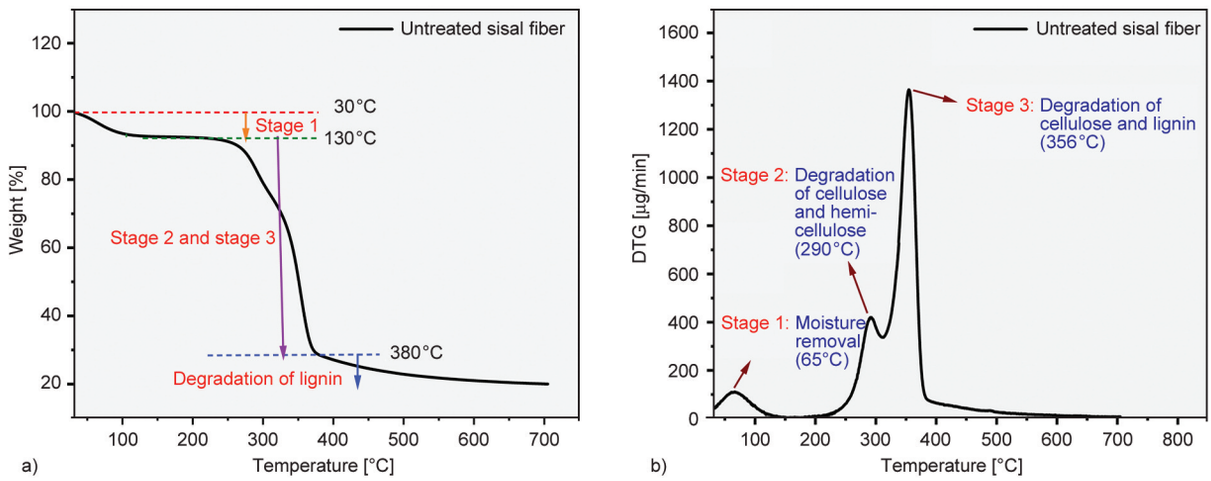

Figure 4. a) TGA and b) DTG curves of untreated sisal fiber.

load transmission. The existence of similar phenomena was observed in the study of bio PBS/PLA/Bamboo fibers based composite materials [29].

It is evident from Figure 5b that the tensile modulus of all PLA/SF and bio PBS/SF composites have a higher value than those of the respective pure matrix. The amount of fiber content in the matrix significantly impacts the increase in tensile modulus. The tensile modulus of PLA/SF composites increased by approximately 14.0, 33.5, and 68.1%, respectively, when 10, 20, and 30 wt% of SF were added to the PLA matrix. Similarly, the tensile modulus of bio PBS/SF composites increased by 8.8, 171.5, and 279.7%, respectively. The addition of stiff SFs improves the stiffness of the polymer composite. As developed composites are rigid, a given quantity of strain within

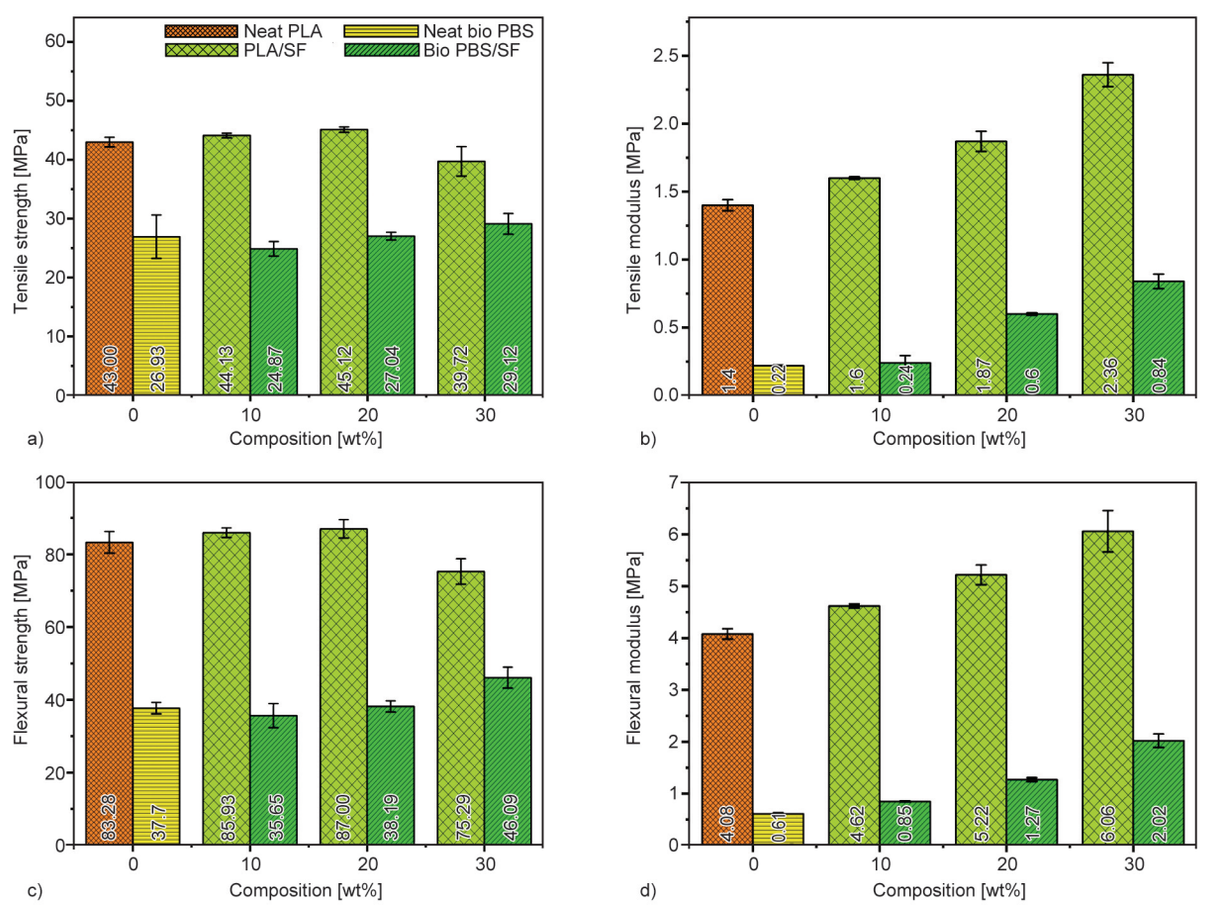

Figure 5. a), b) Tensile and c), d) flexural properties of biocomposites.

elastic limits necessitates higher tension. As a result, the tensile modulus of composites increased [30].

3.4.2. Flexural properties

The flexural properties of PLA/SF and bio PBS/SF composites were evaluated under a three-point bending load, and the results are shown in Figures 5c and 5d. The maximum flexural strength values of the PLA/SF and bio PBS/SF composites were 87.00 MPa (at 20SF/PLA) and 46.09 MPa (at 30SF/bio PBS), respectively, demonstrating good stiffness and higher rigidity. The flexural modulus significantly increased as the fiber content increased. An enhancement of 48.4% (with 30 wt% of SF) and 228.5% (with 30 wt% of SF) was found to be the maximum in SF/PLA and SF/bio PBS composites, respectively. Compared to bio PBS/SF biocomposites, PLA/SF biocomposites have less percentage change in tensile and flexural characteristics. This difference might be attributed to SF/bio PBS composites having better interfacial bonding and good processability with sisal fibers than SF/PLA composites.

3.4.3. Impact strength

As depicted in Table 2, the results reveal that fiber loading reduced the impact resistance of the developed biocomposites. The lower interfacial strength between matrix and sisal fibers may lead to the low-impact energy absorption of developed composites. The increased fiber loading creates stress concentration sites at the fiber-matrix interface, which leads to decreased impact strength of developed biocomposites [31]. The chemical constituents, matrix characteristics, interfacial bond strength between the matrix and fiber, and the void content significantly influence the impact strength of biocomposites.

3.5. Morphological analysis of developed composites

The SEM images of fractured surfaces after tensile testing of the SF/bio PBS and SF/PLA composites are depicted in Figure 6. In Figure 6, the first three images (Figures 6a–6c) describe the morphology of SF/bio PBS composites with 10, 20, and 30 wt% fiber content, respectively. Similarly, the last three pictures (Figures 6d–6f) describe the morphology of SF/PLA composites. The SEM micrograph (Figure 6c) of the 30SF/bio PBS composite has shown better fiber-matrix interaction when compared to 10 and 20 wt% SF/bio PBS composites. The strong fiber-matrix interaction promotes load transfer between the matrix and untreated sisal fiber. Also, Figure 6c shows fiber breakage. Fiber breakage is only conceivable when strong interfacial adhesion exists between the matrix and fiber. On the other hand, as seen in the 10SF/bio PBS composite (Figure 6a), weak interfacial bonding (fiber debonding) inevitably leads to fiber pull-outs and voids. However, fewer fiber pull-outs were observed in 30SF/bio PBS composite (Figure 6c), proving that 30 wt% of sisal fiber loading has good compatibility with bio PBS [32].

The mode of fracture of composites made of 10SF/PLA, 20SF/PLA, and 30SF/PLA under tensile loading is depicted in Figures 6d, 6e, and 6f, respectively. The absence of adequate adhesion between the constituents in the composites leads to fiber pull-outs, as we can observe in 10 and 30 wt% SF/PLA composites [30]. These micrographs also revealed voids, fiber bending, and PLA matrix cracking (due to stress concentration). 30SF/PLA (Figure 6f) has demonstrated a weaker fiber-matrix interface than its counterparts. In the case of 10SF/PLA and 30SF/PLA composites, weak interfacial bonding inevitably causes

Table 2. Mechanical properties of developed composites.

Composition	Tensile strength [MPa]	Tensile modulus [GPa]	Flexural strength [MPa]	Flexural modulus [GPa]	Impact strength [J/m]
Neat PLA	43.00±3.81	1.40±0.04	83.28±2.97	4.08±0.10	74.28±1.34
10SF_PLA	44.13±0.40	1.60±0.01	85.93±1.31	4.62±0.04	33.70±1.50
20SF_PLA	45.12±0.47	1.87±0.07	87.00±2.54	5.22±0.19	44.34±2.75
30SF_PLA	39.72±2.51	2.36±0.08	75.29±3.50	6.06±0.40	54.30±0.80
Neat bio PBS	26.93±3.68	0.22±0.01	37.70±1.58	0.61±0.02	87.75±1.17
10SF_bio PBS	24.87±1.24	0.24±0.05	35.65±3.33	0.85±0.01	38.74±3.57
20SF_bio PBS	27.04±0.65	0.60±0.01	38.19±1.52	1.27±0.04	48.16±3.00
30SF_bio PBS	29.12±1.75	0.84±0.05	46.09±2.87	2.02±0.13	72.14±9.93

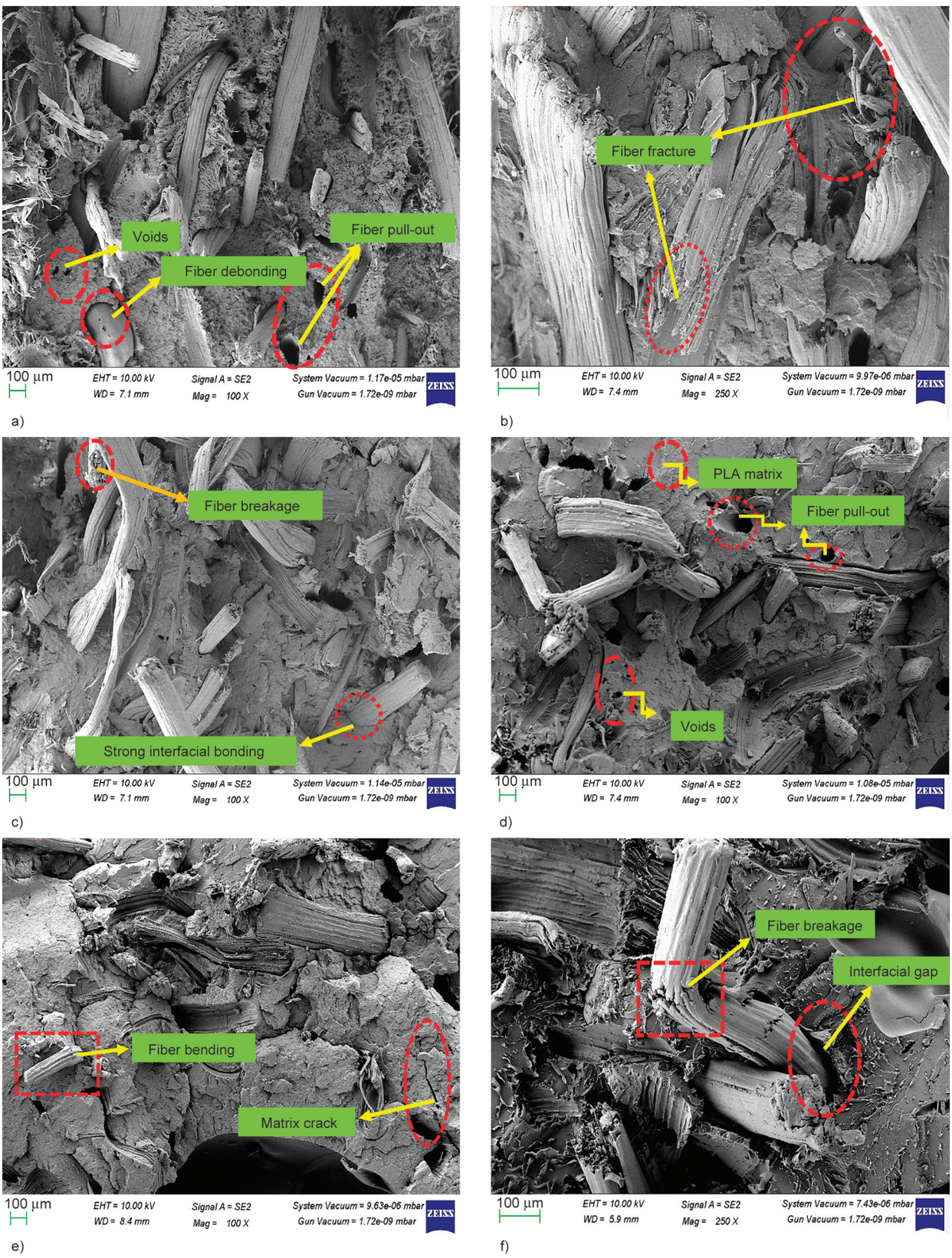

Figure 6. SEM images of a)–c) SF/bio PBS and d)–f) SF/PLA biocomposites after tensile testing.

fiber pull-outs and voids, leading to poor mechanical properties.

From the SEM micrographs, we can observe that 30SF/bio PBS (Figure 6c) and 20SF/PLA (Figure 6e) have shown better results than their counterparts, which was also substantiated by respective mechanical properties and degree of crystallinity of these composites.

3.6. Thermal properties of biocomposites

The weight loss of the biocomposites varies according to temperature, as demonstrated in Figures 7a and 7d. The thermal degradation pattern is consistent across all biocomposites. Due to the inclusion of sisal fibers into the matrix, the thermal degradation temperature of the developed biocomposites was slightly reduced. This may be because the relative molecular mass of the matrix was reduced, and the amount of the fibers increased leading to higher cellulose, hemicellulose, and lignin content in the composites. Since these chemical constituents of fiber are prone to thermal degradation, therefore, a decrease in the degradation temperature of biocomposites was

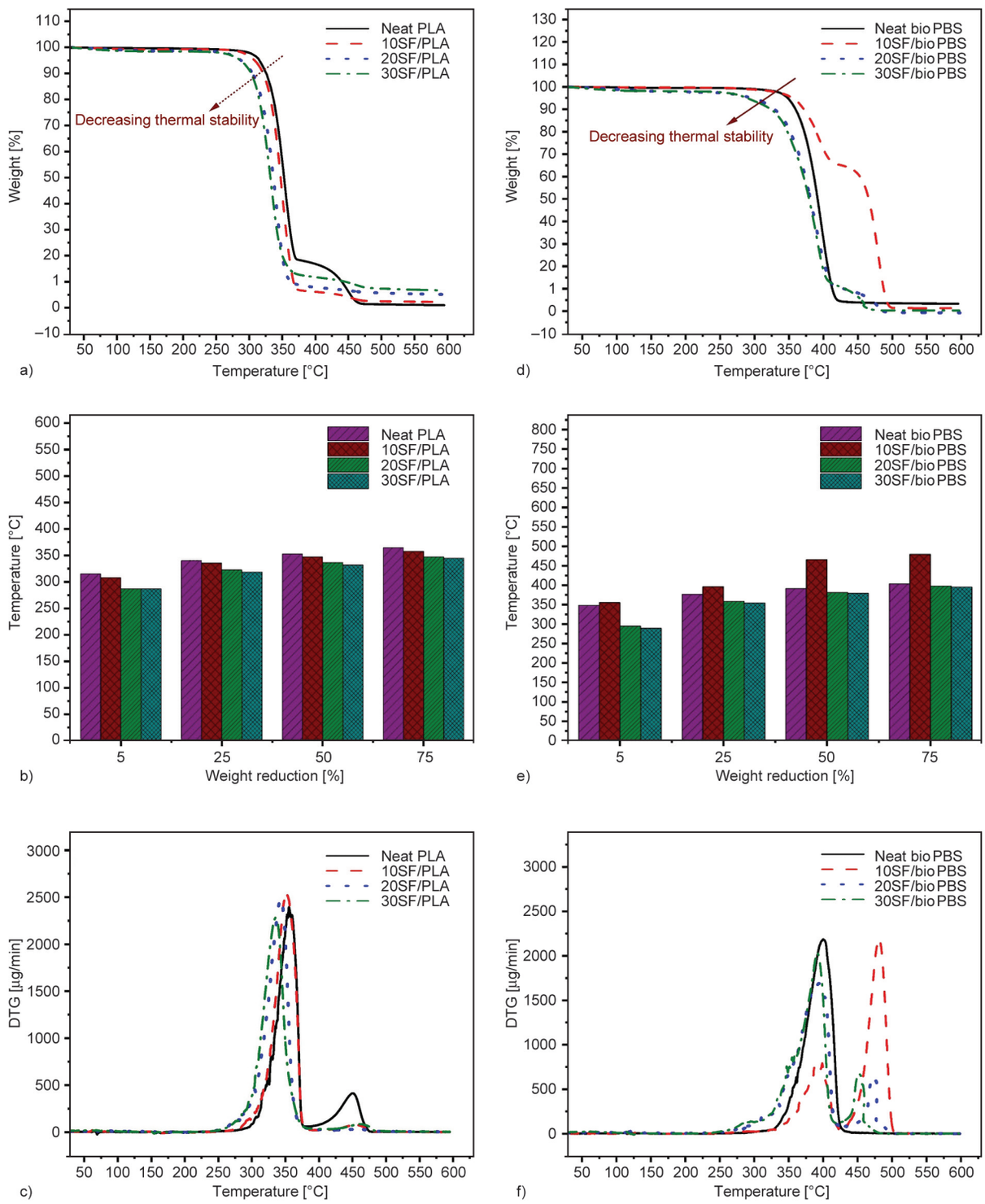

Figure 7. TGA (a), (d), weight reduction (b), (e), and DTG graphs (c), (f) for SF/PLA and SF/bio PBS composites, respectively.

observed [33]. In Figures 7b and 7e, a graphic representation of the weight loss [%] with the temperature is shown. It can be seen that, at the temperature ranges of 287–316, 318–340, 332–353, and 345–365 °C, respectively, all SF/PLA biocomposites lost 5, 25, 50, and 75% of their weight.

Similarly, in the case of SF/bio PBS composites, temperature ranges for similar weight loss [%] are 289–355, 355–397, 379–466, and 395–480 °C, respectively. From the results, it can be observed that SF/bio PBS biocomposites have better thermal stability than SF/PLA composites. Figure 7d shows the weight loss curves for the SF/bio PBS composites. Results showed that up to 200 °C, biocomposites had similar thermal stability as the pristine matrix. However, the thermal degradation behavior changed significantly when sisal fiber concentration increased to 30 wt% due to the lower thermal stability of constituents (cellulose, hemicellulose) of fibers [33]. The weight loss of the developed biocomposites with respect to temperature variation is categorized into three stages. The weight loss at 75–160 °C (SF/PLA composites) and 75–190 °C (SF/bio PBS composites) is related to moisture evaporation in the SF. Weight loss in the temperature range of 370 and 471 °C for SF/PLA composites and between 420 and 493 °C for SF/bio PBS composites is attributable to the pyrolysis of residual lignin and the pyrolysis of the matrix [33]. The peak in DTG curves for the SF/PLA and SF/bio PBS composites are depicted in Figures 7c and 7f, respectively. The highest weight loss was recorded between 255 and 370 °C for SF/PLA composites and between 250 and 420 °C for SF/bio PBS composites, representing the pyrolysis of the matrix and hemicellulose as well as cellulose present in the fibers. A comparable thermal disintegration pattern was determined for all biocomposites, indicating that thermal degradation behavior is not significantly impacted by fiber loading in the case of the developed composites. Figure 7f demonstrates that the virgin bio PBS only exhibits one degradation stage in the DTG profile, whereas composites exhibit two degradation steps. The degradation of the sisal fibers causes the first degradation to occur at 290 °C, while the degradation of the bio PBS matrix is responsible for the second degradation, which occurs at 401 °C [31, 35]. In the case of SF/bio PBS composites, the introduction of fibers resulted in a new interface (between fiber-matrix) which results in a change of thermal degradation mechanism, and therefore, the developed composites depicted two degradation peaks. Regarding the 10SF/bio PBS composite, we can observe the intense peak similar to the neat PBS degradation peak stated that 10SF/bio PBS follows the pristine PBS degradation process rather than the composite degradation process because 10SF/bio PBS has inadequate fiber content to be compatible with bio PBS. This is also evidence of decreased mechanical properties at 10SF/bio PBS. TGA and DTG results can be used to select operating conditions for the fabrication of biocomposite products. It is necessary to keep the processing temperature below 250 °C to prevent the thermal deterioration of developed biocomposites.

3.7. XRD analysis

The characteristics of biocomposites are substantially influenced by the crystallinity level. XRD analysis was used to assess the effect of sisal fiber loading on the crystallinity of the biocomposites. The XRD spectra for the surface of biocomposites are displayed in Figure 8. The software (Origin 2022b) was adopted

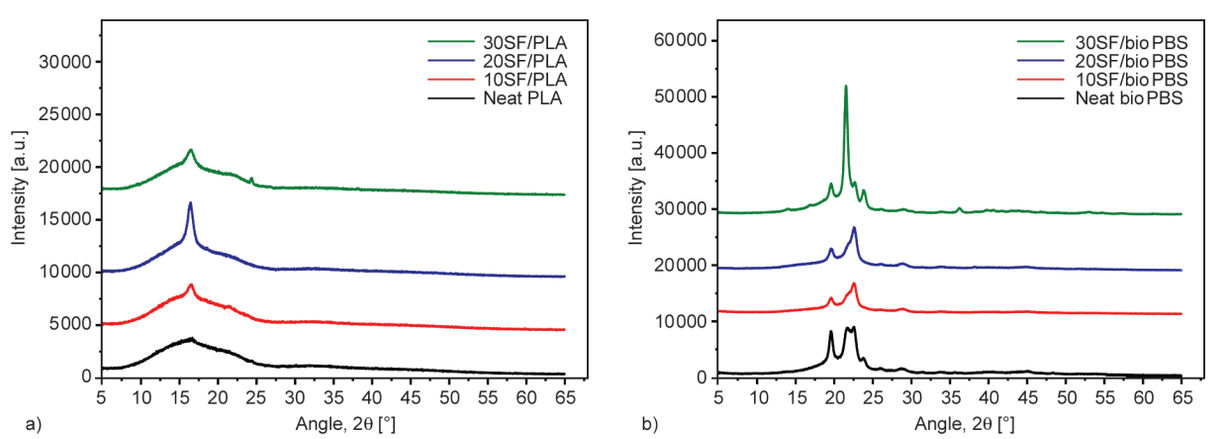

Figure 8. XRD spectra of a) SF/PLA and b) SF/bio PBS biocomposites.

to interpret the obtained data and calculate the total and crystalline area under the curve. The XRD patterns of pure PLA and SF/PLA green composites are shown in Figure 8a. XRD patterns of virgin PLA exhibit only one broad peak without sharp peaks at about $2\theta = 16.44°$. In the XRD spectra of SF/PLA composites, a single diffraction peak is detected, and the strength of this peak is ascertained to be greater and sharper than that of virgin PLA, suggesting increased crystallinity. In SF/PLA composites, comprising 10 to 30 wt% SF, the degree of crystallinity was almost 14.77, 17.88, and 16.81%, respectively [30, 36]. As illustrated in Figure 8b, the XRD for bio PBS provides three diffraction peaks at 19.6°, 21.71°, and 22.56° (with a variation of about ±0.2° [37]). The inclusion of fibers encourages structural alterations, and plane peaks frequently merge and change intensities [37]. From the results, the crystallinity index of pristine bio PBS was 37.03%, which was identified as a semi-crystalline polymer [38]. A degree of crystallinity of almost 33.04, 34.84, and 41.13% was obtained in SF/bio PBS composites comprising 10, 20, 30 wt% SF, respectively. Significant peaks between 16.44° and 22.56° in these composites confirm the existence of cellulose-I (existed between the fiber-matrix interface), proving the polymorphic nature of the composite structure. An interface between the fibers and the matrix can be created during extrusion as fibers and polymer pellets are compounded. Subsequent processing (injection molding) can improve the interfacial characteristics between constituents, increasing the crystallinity of composites. Compared to their counterparts, the crystallinity of the 20SF/PLA (20 wt% SF with PLA matrix) and 30SF/bio PBS (30 wt% SF with bio PBS matrix) biocomposites was found to be the highest. Generally, in plant fibers, cellulose is made of hydrocarbons, which determine the crystallinity of fibers and provide strength and stiffness because cellulose itself acts as a reinforcement in microfibrils of fibers. In biocomposites, natural fibers act as nucleating agents, changing composites' structural order. Therefore, cellulose and hemicellulose content in fibers affect the crystallinity and subsequently the mechanical and thermal properties of biocomposites.

3.8. DMA results

Figure 9 depicts the temperature-dependent variation of storage modulus (E'), loss modulus (E''), and tan δ of the SF/PLA and SF/bio PBS composites. Figures 9a and 9d have shown the temperature-dependent areas where the physical state of the neat polymers and their biocomposites has changed. The polymer and its biocomposites are often rigid and hard in the glassy zone (in the case of SF/bio PBS composites, the measurement starts at a temperature lower than –45 °C so that we can observe a very narrow region in Figure 9d). Beyond this zone, the material starts deforming due to increased temperature. Hence the behavior of the material has changed. At room temperature (around 30 °C), PLA is hard and brittle because it is in a glassy region, whereas bio PBS is soft and ductile as it is in the rubbery zone.

From Figures 9a and 9d, when SF is added to the matrix, E' significantly improves, which may be attributed to the better stress transfer efficiency between fiber and matrix [34]. The greater the value of E', the more rigid the material and the lower its deformation capacity. The movement of polymer molecular units and side groups is closely correlated with E' values [19]. The findings show that the E' values for all composite specimens are higher in the glassy region (rigid zone) since the material is hard and has lower deformation capacity in the glassy region, resulting in significant resistance to movement in the molecular chain. As the temperature increases, the values of E' slowly decline because of the reduction of stiffness in the fiber and improved molecular mobility of biopolymeric chains (increased temperature weakens the intramolecular bond strength of polymeric chains) [39]. At ambient temperature, SF/PLA composites are in the glassy region, whereas SF/bio PBS composites are in the rubbery zone and are ductile at room temperature. A sudden fall in E' was recorded for the SF/PLA specimens and SF/bio PBS specimens, respectively, in the temperature ranges of 55 to 65 °C and –45 to 0 °C, corresponding to a reduction in stiffness at the glass transition zone (T_g) [40, 41]. The 20SF/PLA (14232.69 MPa) and 30SF/bio PBS (11749.10 MPa) composites have higher storage modulus than their counterparts, associated with enhanced interfacial bonding between composite constituents as a result of the bolstering of interfaces. The storage modulus of 20SF/PLA and 30SF/bio PBS composites was almost 67 and 170% higher than the E' of the PLA matrix and bio PBS matrix, respectively. Furthermore, an increase in crystallinity could contribute to the growth in the storage modulus of the 20SF/PLA and 30SF/bio PBS composites. The increase in crystallinity

indicates a rise in the number of crystalline regions in the composites, which could serve as reinforcement or cross-linking for the amorphous areas, increasing the load-bearing properties of the 20SF/PLA and 30SF/bio PBS composites.

The viscous reaction of a substance is usually referred to as the loss modulus (E''). It concerns the movement of polymeric chains in composites that have been produced. Figures 9b and 9e show that the loss modulus of 30SF/PLA (2238.87 MPa) and 30SF/bio PBS (808.63 MPa) composites are significantly higher than that of virgin polymers. The mobility of polymer molecular chains is impeded and causes a rise in the viscosity of biocomposites because

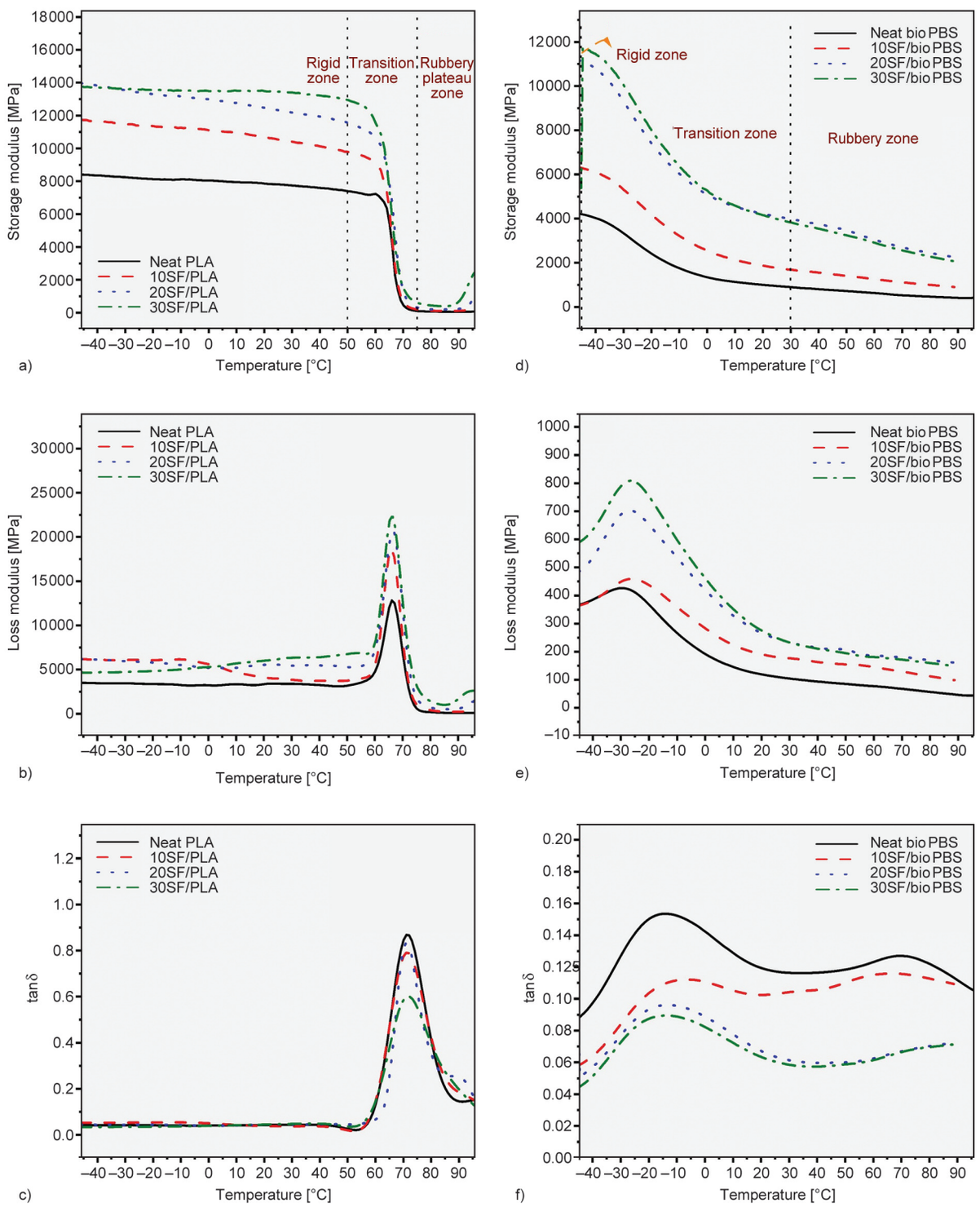

Figure 9. Storage modulus (a), (d), loss modulus (b), (e), and tan δ (c), (f) for SF/PLA and SF/bio PBS composites, respectively.

fibers increase stiffness and restrict the movement of polymeric chains in the composites [30]. The loss modulus of the 30SF/PLA and 30SF/bio PBS composites was around 74 and 89% greater than the loss modulus of the PLA matrix and the bio PBS matrix, respectively. Interfacial bonding between PLA and SF is low compared to bio PBS and SF. Hence, the increased percentile change in the loss modulus was more in SF/bio PBS composites.

Tan δ is also known as the damping coefficient or the loss factor. The loss factor is shown in Figures 9c and 9f as a function of temperature. The peak in the curves for each developed composite decreased compared to virgin polymers. It could be owing to the integration of SF, which leads to an interaction of the matrix and fiber, restricting the motion of polymeric chains. The tan δ peak height is commonly used to evaluate the damping capabilities of composites. Tan δ values for pure PLA and pure bio PBS are 0.868 and 0.153, respectively. On the other hand, the tan δ peak of the composite decreases with the addition of sisal fibers, which is due to interfacial interaction between the matrix and the fibers, inhibiting molecular mobility.

According to the results of DMA, it is evident that the increased percentile changes in E' and E'' values of SF/bio PBS composites were more than the SF/PLA composites. It is because the fibers and matrix have strong interfacial bonds and minimal defects during the fabrication of these types of composites, as observed in SEM analysis also.

4. Conclusions

The potential of sisal fiber as reinforcement for developing biodegradable SF/PLA and SF/bio PBS thermoplastic composites was experimentally investigated. The current research findings suggest that sisal fibers can be successfully incorporated into PLA and bio PBS biodegradable polymers to produce biocomposites. Extrusion-injection molding was used to fabricate SF/PLA and SF/bio PBS biocomposites with fiber content varying from 10 to 30 wt%. The primary conclusions of the current investigation are as follows;

- The maximum tensile and flexural strength of the SF/PLA and SF/bio PBS composites were observed at 20 and 30 wt% of fiber loading, respectively. On the other hand, the tensile and flexural modulus of developed composites increased with an increase in fiber loading from 10 to 30 wt% because the incorporation of rigid sisal fibers enhanced the modulus of biocomposites.
- The sisal fiber loading influences the thermal characteristics of developed composites because increased fiber loading results in increased cellulose and hemicellulose content in composites, which is thermally unstable at elevated temperatures.
- The degree of crystallinity of the 20SF/PLA (17.88%) and 30SF/bio PBS (41.13%) biocomposites was recorded to be maximum which consequently also led to the better mechanical properties of these composites.
- The SEM images have shown better fiber-matrix interfacial bonding for 20 and 30 wt% of the sisal fiber content for SF/PLA and SF/bio PBS composites, respectively. Fiber breakage was the major failure mechanism observed indicating good adhesion between PLA/bio PBS and the sisal fibers.
- The storage and loss modulus of developed composites increased with fiber loading from 10 to 30 wt%. The increased percentile change in mechanical, crystallinity, and DMA properties of SF/bio PBS composites was found to be higher than SF/PLA composites as compared to the neat polymers.

Additionally, it has been concluded that short-sisal fiber-based biocomposites have enormous potential for usage in various lightweight, secondary load-bearing, and non-structural applications, including dashboards, door panels, and other interior parts of automobiles. The produced biocomposites can also be used as paperweights, phone cases, and mirror casings. Thus for ensuring widespread commercial application of sustainable composite materials, the optimization of the fiber loading and development of good quality, cost-effective fabrication/processing techniques is necessary.

Acknowledgements

The authors would like to acknowledge the financial support provided by the Ministry of Education (MoE), Government of India.

References

[1] Nanni A., Messori M.: Thermo-mechanical properties and creep modelling of wine lees filled polyamide 11 (PA11) and polybutylene succinate (PBS) bio-composites. Composite Science and Technology, **188**, 107974 (2020). https://doi.org/10.1016/j.compscitech.2019.107974

[2] Song H., Lee S. Y.: Production of succinic acid by bacterial fermentation. Enzyme and Microbial Technology, **39**, 352–361 (2006). https://doi.org/10.1016/j.enzmictec.2005.11.043

[3] Zeikus J. G., Jain M. K., Elankovan P.: Biotechnology of succinic acid production and markets for derived industrial products. Applied Microbiology and Biotechnology, **51**, 545–552 (1999). https://doi.org/10.1007/s002530051431

[4] Yim H., Haselbeck R., Niu W., Pujol-Baxley C., Burgard A., Boldt J., Khandurina J., Trawick J. D., Osterhout R. E., Stephen R., Estadilla J., Teisan S., Schreyer H. B., Andrae S., Yang T. H., Lee S. Y., Burk M. J., Van Dien S.: Metabolic engineering of *Escherichia coli* for direct production of 1,4-butanediol. Nature Chemical Biology, **7**, 445–452 (2011). https://doi.org/10.1038/nchembio.580

[5] Aeschelmann F., Carus M.: Biobased building blocks and polymers in the world: Capacities, production, and applications-status quo and trends towards 2020. Industrial Biotechnology, **11**, 154–159 (2015). https://doi.org/10.1089/ind.2015.28999.fae

[6] Xu L., Zhao J., Qian S., Zhu X., Takahashi J.: Green-plasticized poly(lactic acid)/nanofibrillated cellulose biocomposites with high strength, good toughness and excellent heat resistance. Composites Science and Technology, **203**, 108613 (2021). https://doi.org/10.1016/j.compscitech.2020.108613

[7] Silva C. G., Campini P. A. L., Rocha D. B., Rosa D. S.: The influence of treated eucalyptus microfibers on the properties of PLA biocomposites. Composites Science and Technology, **179**, 54–62 (2019). https://doi.org/10.1016/j.compscitech.2019.04.010

[8] Yusoff R. B., Takagi H., Nakagaito A. N.: Tensile and flexural properties of polylactic acid-based hybrid green composites reinforced by kenaf, bamboo and coir fibers. Industrail Crops and Products, **94**, 562–573 (2016). https://doi.org/10.1016/j.indcrop.2016.09.017

[9] Mtibe A., Motloung M. P., Bandyopadhyay J., Ray S. S.: Synthetic biopolymers and their composites: Advantages and limitations – An overview. Macromolecular Rapid Communications, **42**, 2100130 (2021). https://doi.org/10.1002/marc.202100130

[10] Verma D., Fortunati E.: Biopolymer processing and its composites: An introduction. in 'Biomass, biopolymer-based materials and bioenergy' (eds.: Verma D., Fortunati E., Jain S., Zhang X.) Woodhead, Sawston, 3–23 (2019). https://doi.org/10.1016/B978-0-08-102426-3.00001-1

[11] Fiore V., Scalici T., Nicoletti F., Vitale G., Prestipino M., Valenza A.: A new eco-friendly chemical treatment of natural fibres: Effect of sodium bicarbonate on properties of sisal fibre and its epoxy composites. Composites Part B: Engineering, **85**, 150–160 (2016). https://doi.org/10.1016/j.compositesb.2015.09.028

[12] Bekele A. E., Lemu H. G., Jiru M. G.: Experimental study of physical, chemical and mechanical properties of enset and sisal fibers. Polymer Testing, **106**, 107453 (2022). https://doi.org/10.1016/j.polymertesting.2021.107453

[13] Thomas B. C., Jose Y. S.: A study on characteristics of sisal fiber and its performance in fiber reinforced concrete. Materials Today: Proceedings, **51**, 1238–1242 (2022). https://doi.org/10.1016/j.matpr.2021.07.312

[14] Pantaloni D., Rudolph A. L., Shah D. U., Baley C., Bourmaud A.: Interfacial and mechanical characterisation of biodegradable polymer-flax fibre composites. Composites Science and Technology, **201**, 108529 (2021). https://doi.org/10.1016/j.compscitech.2020.108529

[15] Ngaowthong C., Borůvka M., Běhálek L., Lenfeld P., Švec M., Dangtungee R., Siengchin S., Rangappa S. M., Parameswaranpillai J.: Recycling of sisal fiber reinforced polypropylene and polylactic acid composites: Thermo-mechanical properties, morphology, and water absorption behavior. Waste Management, **97**, 71–81 (2019). https://doi.org/10.1016/j.wasman.2019.07.038

[16] Zhu Z., Hao M., Zhang N.: Influence of contents of chemical compositions on the mechanical property of sisal fibers and sisal fibers reinforced PLA composites. Journal of Natural Fibers, **17**, 101–112 (2020). https://doi.org/10.1080/15440478.2018.1469452

[17] Feng Y-H., Zhang D-W., Qu J-P., He H-Z., Xu B-P.: Rheological properties of sisal fiber/poly(butylene succinate) composites. Polymer Testing, **30**, 124–130 (2011). https://doi.org/10.1016/j.polymertesting.2010.11.004

[18] Bajpai P. K., Singh I., Madaan J.: Comparative studies of mechanical and morphological properties of polylactic acid and polypropylene based natural fiber composites. Journal of Reinforced Plastics and Composites, **31**, 1712–1724 (2012). https://doi.org/10.1177/0731684412447992

[19] Yan X., Liu C., Qiao L., Zhu K., Tan H., Dong S., Lin Z.: Crystallization and dynamic mechanical behavior of coir fiber reinforced poly(butylene succinate) biocomposites. Journal of Renewable Materials, **10**, 1039–1048 (2022). https://doi.org/10.32604/JRM.2022.017239

[20] Li Y., Sang L., Wei Z., Ding C., Chang Y., Chen G., Zhang W., Liang J.: Mechanical properties and crystallization behavior of poly(butylene succinate) composites reinforced with basalt fiber. Journal of Thermal Analysis and Calorimetry, **122**, 261–270 (2015). https://doi.org/10.1007/s10973-015-4732-8

[21] Samouh Z., Molnar K., Boussu F., Cherkaoui O., El Moznine R.: Mechanical and thermal characterization of sisal fiber reinforced polylactic acid composites. Polymers for Advanced Technologies, **30**, 529–537 (2019). https://doi.org/10.1002/pat.4488

[22] Naik T. P., Gairola S., Singh I., Sharma A. K.: Microwave hybrid heating for moulding of sisal/jute/HDPE composites. Journal of Natural Fibers, **19**, 13524–13538 (2022).
https://doi.org/10.1080/15440478.2022.2100553

[23] Silveira M. V., dos Santos Ferreira J. W., Casagrande M. D. T.: Effect of surface treatment on natural aging and mechanical behavior of sisal fiber–reinforced sand composite. Journal of Materials in Civil Engineering, **34**, 1–11 (2022).
https://doi.org/10.1061/(asce)mt.1943-5533.0004237

[24] Gudayu A. D., Steuernagel L., Meiners D., Gideon R.: Effect of surface treatment on moisture absorption, thermal, and mechanical properties of sisal fiber. Journal of Industrial Textiles, **51**, 2853S–2873S (2022).
https://doi.org/10.1177/1528083720924774

[25] Chaitanya S., Singh I.: Sisal fiber-reinforced green composites: Effect of ecofriendly fiber treatment. Polymer Composites, **39**, 4310–4321 (2018).
https://doi.org/10.1002/pc.24511

[26] Ye C., Ma G., Fu W., Wu H.: Effect of fiber treatment on thermal properties and crystallization of sisal fiber reinforced polylactide composites. Journal of Reinforced Plastics and Composites, **34**, 718–730 (2015).
https://doi.org/10.1177/0731684415579090

[27] Rajesh G., Ratna Prasad A. V., Gupta A. V. S. S. K. S.: Mechanical and degradation properties of successive alkali treated completely biodegradable sisal fiber reinforced poly lactic acid composites. Journal of Reinforced Plastics and Composites, **34**, 951–961 (2015).
https://doi.org/10.1177/0731684415584784

[28] Sachin S. R., Kannan T. K., Rajasekar R.: Effect of wood particulate size on the mechanical properties of PLA biocomposite. Pigment & Resin Technology, **49**, 465–472 (2020).
https://doi.org/10.1108/PRT-12-2019-0117

[29] Rasheed M., Jawaid M., Parveez B.: Preparation, characterization and properties of biodegradable composites from bamboo fibers – Mechanical and morphological study. Journal of Polymers and the Environment, **29**, 4120–4126 (2021).
https://doi.org/10.1007/s10924-021-02158-7

[30] Pujar N. M., Mani Y.: Development and characterization of pigeon pea stalk fiber reinforced polylactic acid sustainable composites. Journal of Natural Fibers, **19**, 15637–15652 (2022).
https://doi.org/10.1080/15440478.2022.2131684

[31] Pivsa-Art S., Pivsa-Art W.: Eco-friendly bamboo fiber-reinforced poly(butylene succinate) biocomposites. Polymer Composites, **42**, 1752–1759 (2021).
https://doi.org/10.1002/pc.25930

[32] Nam T. H., Ogihara S., Nakatani H., Kobayashi S., Song J. I.: Mechanical and thermal properties and water absorption of jute fiber reinforced poly(butylene succinate) biodegradable composites. Advanced Composite Materials, **21**, 241–258 (2012).
https://doi.org/10.1080/09243046.2012.723362

[33] Gairola S., Sinha S., Singh I.: Novel millet husk crop-residue based thermoplastic composites: Waste to value creation. Industrial Crops and Products, **182**, 114891 (2022).
https://doi.org/10.1016/j.indcrop.2022.114891

[34] Komal U. K., Lila M. K., Singh I.: PLA/banana fiber based sustainable biocomposites: A manufacturing perspective. Composites Part B: Engineering, **180**, 107535 (2020).
https://doi.org/10.1016/j.compositesb.2019.107535

[35] Gowman A., Wang T., Rodriguez-Uribe A., Mohanty A. K., Misra M.: Bio-poly(butylene succinate) and its composites with grape pomace: Mechanical performance and thermal properties. ACS Omega, **3**, 15205–15216 (2018).
https://doi.org/10.1021/acsomega.8b01675

[36] Kaavessina M., Ali I., Al-Zahrani S. M.: The influences of elastomer toward crystallization of poly(lactic acid). Procedia Chemistry, **4**, 164–171 (2012).
https://doi.org/10.1016/j.proche.2012.06.023

[37] Platnieks O., Gaidukovs S., Thakur V. K., Barkane A., Beluns S.: Bio-based poly(butylene succinate): Recent progress, challenges and future opportunities. European Polymer Journal, **161**, 110855 (2021).
https://doi.org/10.1016/j.eurpolymj.2021.110855

[38] Bhattacharjee S. K., Chakraborty G., Kashyap S. P., Gupta R., Katiyar V.: Study of the thermal, mechanical and melt rheological properties of rice straw filled poly (butylene succinate) bio-composites through reactive extrusion process. Journal of Polymers and the Environment, **29**, 1477–1488 (2021).
https://doi.org/10.1007/s10924-020-01973-8

[39] Kumar S., Zindani D., Bhowmik S.: Investigation of mechanical and viscoelastic properties of flax- and ramie-reinforced green composites for orthopedic implants. Journal of Materials Engineering and Performance, **29**, 3161–3171 (2020).
https://doi.org/10.1007/s11665-020-04845-3

[40] Saffian H. A., Yamaguchi M., Ariffin H., Abdan K., Kassim N. K., Lee S. H., Lee C. H., Shafi A. R., Alias A. H.: Thermal, physical and mechanical properties of poly(butylene succinate)/kenaf core fibers composites reinforced with esterified lignin. Polymers, **13**, 2359 (2021).
https://doi.org/10.3390/polym13142359

[41] Komal U. K., Lila M. K., Singh I.: Processing of PLA/pineapple fiber based next generation composites. Materials and Manufactuing Processes, **36**, 1677–1692 (2021).
https://doi.org/10.1080/10426914.2021.1942904